Journal of Medicinal Chemistry

Article

Discovery of an SSTR2-targeting maytansinoid conjugate (PEN-221) with potent activity in vitro and in vivo

Brian H. White, Kerry Whalen, Kristina Kriksciukaite, Rossitza G. Alargova, Tsun Au Yeung, Patrick Bazinet, Adam Hale Brockman, Michelle Dupont, Haley Oller, Charles-Andre Lemelin, Patrick Lim Soo, Benoit Moreau, Samantha Perino, James M. Quinn, Gitanjali Sharma, Rajesh Shinde, Beata Sweryda-Krawiec, Richard Wooster, and Mark T. Bilodeau

J. Med. Chem., **Just Accepted Manuscript** • DOI: 10.1021/acs.jmedchem.8b02036 • Publication Date (Web): 08 Feb 2019

Just Accepted

ACS Publications

is published by the American Chemical Society. 1155 Sixteenth Street N.W., Washington, DC 20036

Discovery of an SSTR2-targeting maytansinoid conjugate (PEN-221) with potent activity in vitro and in vivo

Brian H. White, Kerry Whalen, Kristina Kriksciukaite, Rossitza Alargova, Tsun Au Yeung, Patrick Bazinet, Adam Brockman, Michelle DuPont, Haley Oller, Charles-Andre Lemelin, Patrick Lim Soo, Benoît Moreau, Samantha Perino, James M. Quinn, Gitanjali Sharma, Rajesh Shinde, Beata Sweryda-Krawiec, Richard Wooster, Mark T. Bilodeau*

Tarveda Therapeutics, 134 Coolidge Ave. Watertown, MA 02472, U.S.A.

Abstract

Somatostatin receptor 2 (SSTR2) is frequently overexpressed on several types of solid tumors, including neuroendocrine tumors and small cell lung cancer. Peptide agonists of SSTR2 are rapidly internalized upon binding to the receptor and linking a toxic payload

to an SSTR2 agonist is a potential method to kill SSTR2-expressing tumor cells. Herein we describe our efforts towards an efficacious SSTR2-targeting cytotoxic conjugate; examination of different SSTR2 targeting ligands, conjugation sites, and payloads led to the discovery of 22 (PEN-221), a conjugate consisting of microtubule-targeting agent DM1 linked to the C-terminal side chain of Tyr^3-octreotate. PEN-221 demonstrates in vitro activity which is both potent (IC_{50} = 10 nM) and receptor dependent (IC_{50} shifts 90-fold upon receptor blockade). PEN-221 targets high levels of DM1 to SSTR2-expressing xenograft tumors, which has led to tumor regressions in several SSTR2-expressing xenograft mouse models. The safety and efficacy of PEN-221 is currently under evaluation in human clinical trials.

Introduction

Antibody-drug conjugates (ADCs) have shown promise in improving the therapeutic index of anti-cancer agents through selective targeting of active agents to tumor cells while lowering systemic toxicity. The approval of brentuximab vedotin[1], trastuzumab emtansine[2] and inotuzumab ozogamicin[3] have demonstrated the value of antibody-directed therapies in the treatment of patients with cancer. However, despite the clinical

promise ADCs have demonstrated, several challenges preclude their use in the treatment of patients with solid tumors. Solid tumors are frequently poorly vascularized[4] and the rate of diffusion of antibodies through solid tumor tissue is extremely slow[5], which can lead to low levels of ADC uptake within solid tumors[6]. One potential alternative approach to ligand-directed therapies of solid tumors is the use of miniaturized constructs, such as peptide- or small molecule-drug conjugates[7]. While small (>5 kDa) constructs typically suffer from poor pharmacokinetics, their ability to rapidly diffuse through solid tumor tissue frequently allows for extremely high levels of targeted construct uptake into solid tumors[8].

Somatostatin is a peptide hormone produced by paracrine cells within the gastrointestinal tract, lung, and pancreas, and the central nervous system. Somatostatin is produced in two active forms (SST14 and SST28), and the biological effects include neurotransmission, inhibition of gastrointestinal endocrine secretion and cell proliferation. These effects are produced by somatostatin's interaction with five somatostatin receptors (SSTR1-5). While somatostatin itself is cleared within minutes in vivo[9], investigations into peptide analogs of somatostatin have yielded longer-lived peptide analogs selective for all somatostatin receptor subtypes[10]. Of particular note is the peptide analog octreotide[11],

a long-lasting SSTR2 agonist that inhibits secretion of growth hormone through its action at SSTR2 and is approved for use for treatment of acromegaly and symptomatic treatment of patients with carcinoid tumors.

In addition to its role in the endocrine system, SSTR2 is overexpressed on the cell surface of various types of solid tumors, including small-cell lung cancers[12], gastroentero-pancreatic neuroendocrine tumors[13], carcinoids and islet cell tumors[14]. Expression of SSTR2 is limited outside the central nervous system, and since SSTR2 agonists are rapidly internalized into SSTR2-expressing cells upon receptor engagement[15], SSTR2-mediated drug targeting represents a promising method to deliver compounds into SSTR2-expressing tumors[16]. As part of our ongoing effort to explore miniaturized drug conjugates that can rapidly target chemotoxic payloads to solid tumors, we set out to develop an SSTR2-targeted peptide-payload construct that demonstrated SSTR2-mediated cytotoxicity and was able to induce tumor regressions of several different SSTR2-expressing xenografts.

Results and Discussion

Scheme 1. Synthesis of payload/linker combinations

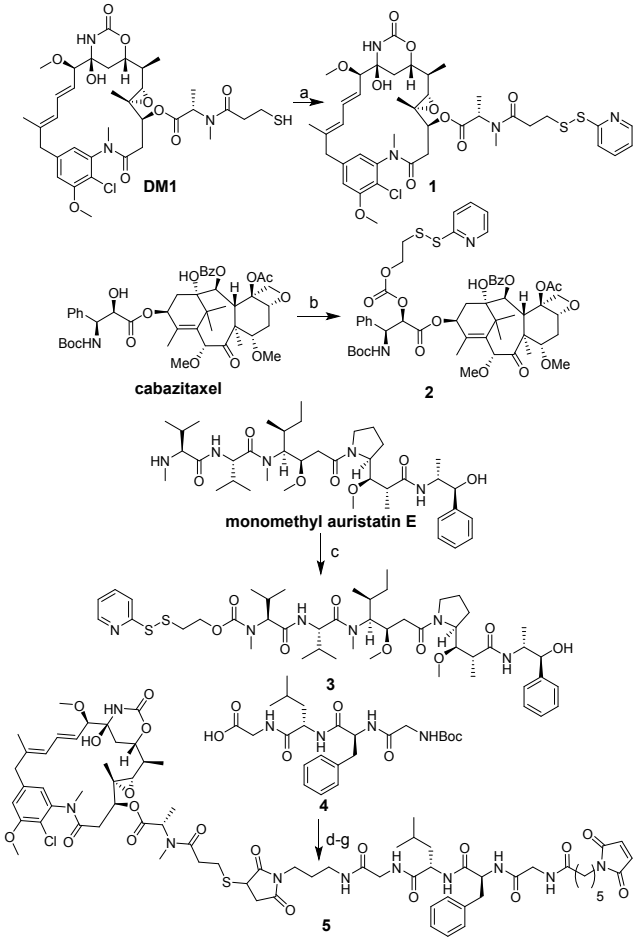

Reagents and conditions: a) 2,2'-dipyridyldisulfide, DMF, AcOH, 0.2M NaOAc; b) 2-(2-pyridinyldithio)ethanol p-nitrophenyl carbonate, DMAP, dichloromethane; (c) 2-(2-pyridinyldithio)ethanol p-nitrophenyl carbonate, DMF, diisopropylethylamine; (d) DCC, HOSu, DMF, 3-aminopropylmaleimide, diisopropylethylamine; (e) TFA; (f) DM1, DMF, pH 5.6 acetate buffer; (g) 6-maleimidohexanoic acid isobuyl carbonic anhydride, DMF, pyridine, 0 °C

Synthesis. Initial conjugates were constructed by linking SSTR2 agonist octreotide to various commercially available chemotoxic payloads. Because of accumulation of the active agent would be limited by number of copies of SSTR2 expressed at the cell surface, potent chemotoxic payloads were examined to ensure that payload delivered via

receptor-mediated endocytosis would be sufficient to kill the tumor cell. Microtubule-targeting agents DM1[17], cabazitaxel[18], and monomethyl auristatin E[19] (MMAE) were selected as potential payloads; synthesis of the corresponding disulfide-linkable constructs **1**, **2**, and **3** are shown in Scheme 1. Because cabazitaxel and MMAE require linking through non-thiol heteroatoms, a disulfide carbonate or carbamate linker[20] was employed for these payloads. In addition, maleimide **5** containing DM1 linked through a lyosomally-cleaved Gly-Phe-Leu-Gly sequence[21] was synthesized.

Scheme 2. Synthesis of octreotide, vapreotide, Tyr^3-octreotate, and cyclic 6-mer conjugates

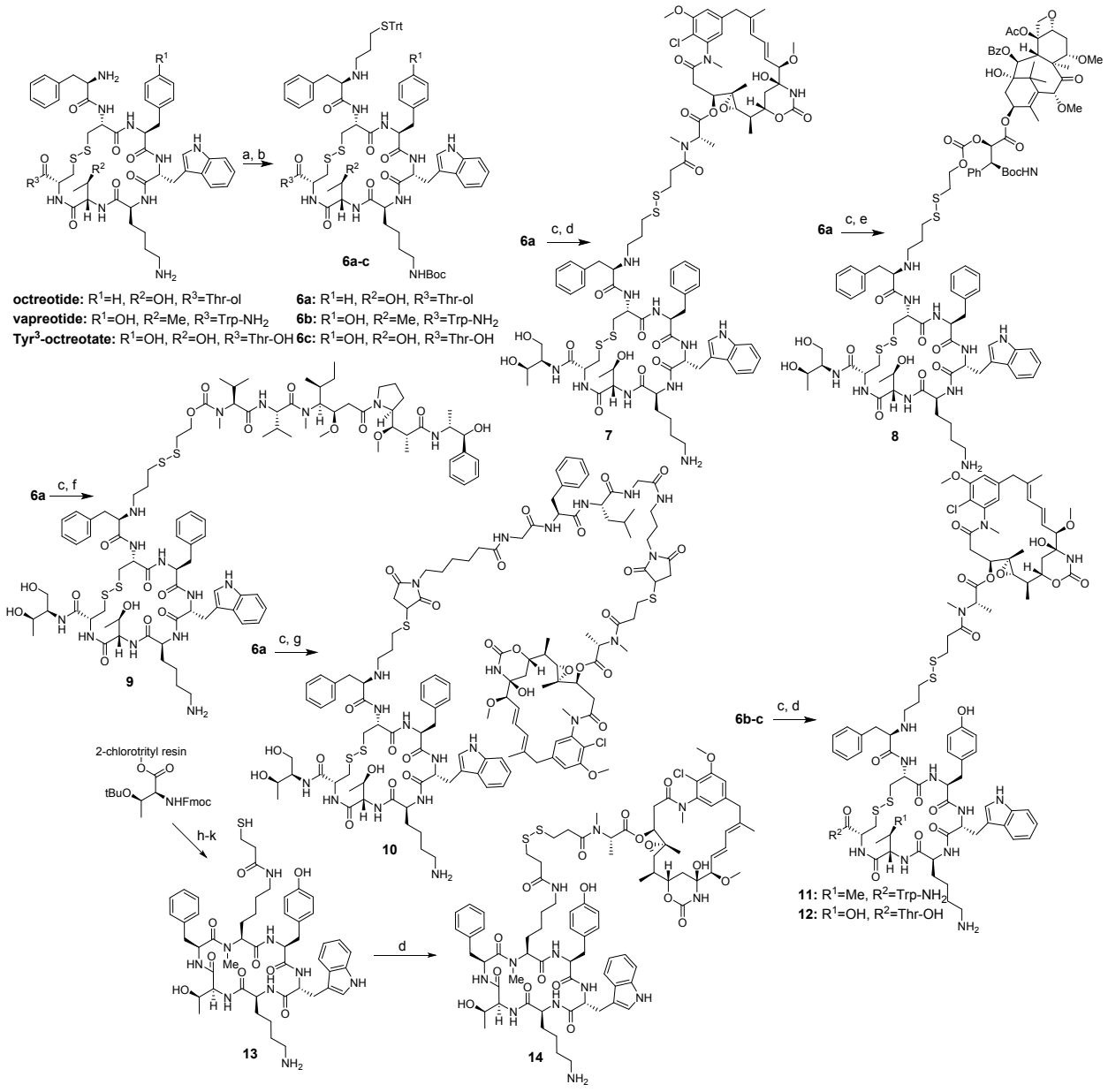

Reagents and conditions: a) BocOSu, DMF, -40 °C to RT; b) S-trityl 3-mercaptopropionaldehyde, $NaBH(OAc)_3$; c) TFA, triisopropylsilane; d) **1**, DMF, pH 7.4 phosphate buffer; e) **2**, DMF, pH 5.6 acetate buffer; f) **3**, DMF, pH 5.6 acetate buffer; g) **5**, DMF, pH 5.6 acetate buffer; h) iterative SPPS with: Nα-Fmoc-Nε-Boc-lysine, Nα-Fmoc-N^{in}-Boc-D-tryptophan, Fmoc-tyrosine(tBu), Nα-Fmoc-Nε-(S-trityl-3-mercaptopropionate)-lysine, Fmoc-phenylalanine; i) 1% TFA in DCM; j) HATU, HOAt, DMF, iPr_2NEt; k) 95:2.5:2.5 TFA:EDT:water

Octreotide was then derivatized with a protected thiol for conjugation to the thiol-reactive payload derivatives (Scheme 2). Selective protection of the lysine side chain with a Boc group, following by reductive amination with S-trityl-3-mercaptopropionaldehyde provided **6a**. Global deprotection and reaction of the free thiol at the N-terminus with the appropriate payload provided DM1 conjugate **7**, cabazitaxel conjugate **8**, MMAE conjugate **9**, and protease-cleavable DM1 conjugate **10**. A protected thiol was appended to the N-terminus of vapreotide[22] and Tyr^3-octreotate analogously to **7**. In addition, cyclic 6-mer peptide **13**[23] with a pendant thiol was made via solid phase synthesis. Conjugation of these ligands with DM1 yielded vapreotide conjugate **11**, Tyr^3-octreotate conjugate **12**, and cyclic 6-mer conjugate **14** respectively.

Scheme 3. Synthesis of Tyr^3-octreotate/DM1 conjugates

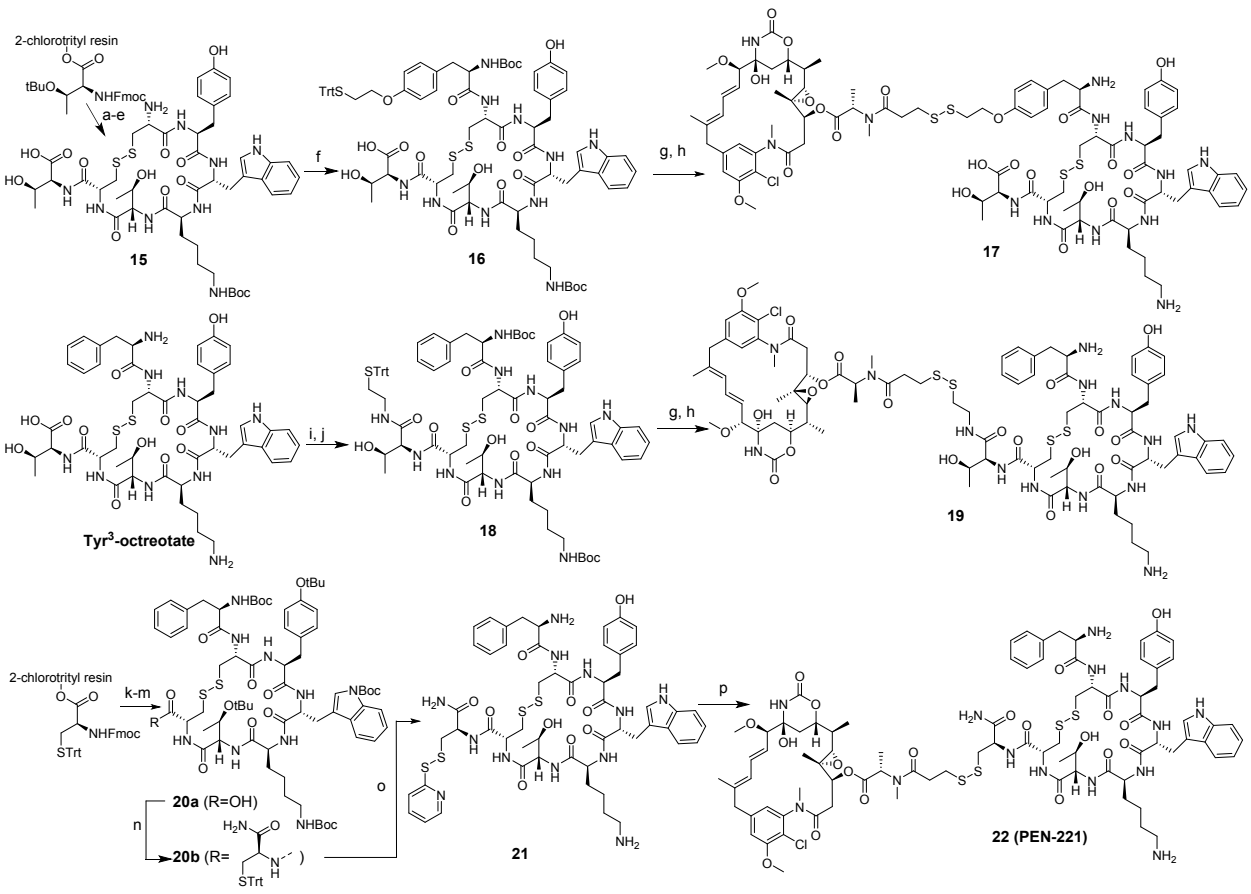

Reagents and conditions: a) iterative SPPS with: Fmoc-S-trityl-cysteine, Fmoc-threonine(tBu), Nα-Fmoc-Nε-Boc lysine, Nα-Fmoc-N^{in}-Boc-D-tryptophan, Fmoc-tyrosine(tBu), Fmoc-S-trityl-cysteine; b) 95:2.5:2.5 TFA:EDT:water; c) I_2, CH_3CN/water; d) Boc_2O, iPr_2NEt, DMF; e) Et_2NH, DCM; f) Boc-O-(S-trityl-2-mercaptoethyl)-D-tyrosine NHS ester, DMF, iPr_2NEt; g) TFA, iPr_3SiH; h) **1**, DMF, iPr_2NEt; i) Boc_2O, DMF, iPr_2NEt; j) S-trityl cysteamine HCl, DMF, HATU, iPr_2NEt; k) iterative SPPS with: Fmoc-threonine(tBu), Nα-Fmoc-Nε-Boc lysine, Nα-Fmoc-N^{in}-Boc-D-tryptophan, Fmoc-tyrosine(tBu), Fmoc-S-trityl-cysteine, Boc-D-phenylalanine; l) I_2, DMF; m) 20% trifluoroethanol in DCM; n) HATU, CH_2Cl_2, S-trityl cysteine amide, iPr_2NEt; o) 2,2'-dithiodipyridine, 1,1,3,3-tetramethyldisiloxane, trifluoroethanol, 12N HCl; p) DM1, THF, pH 3.7 acetate buffer

Additional Tyr^3-octreotate/DM1 conjugates were synthesized by selecting alternative conjugation points on Tyr^3-octreotate that maintained the Tyr-DTrp-Lys-Thr SSTR2

binding pharmacophore (Scheme 3). Thus, Tyr^3-octreotate analogs were synthesized containing protected thiols on the N-terminal side chain (**16**), C-terminus (**18**), or an activated disulfide bond on the C-terminal side chain (**21**). Subsequent conjugation of DM1 provided N-terminal side chain conjugate **17**, the C-terminal conjugate **19**, and the C-terminal side chain conjugate **22**.

Scheme 4. Synthesis of C-terminal side chain conjugates

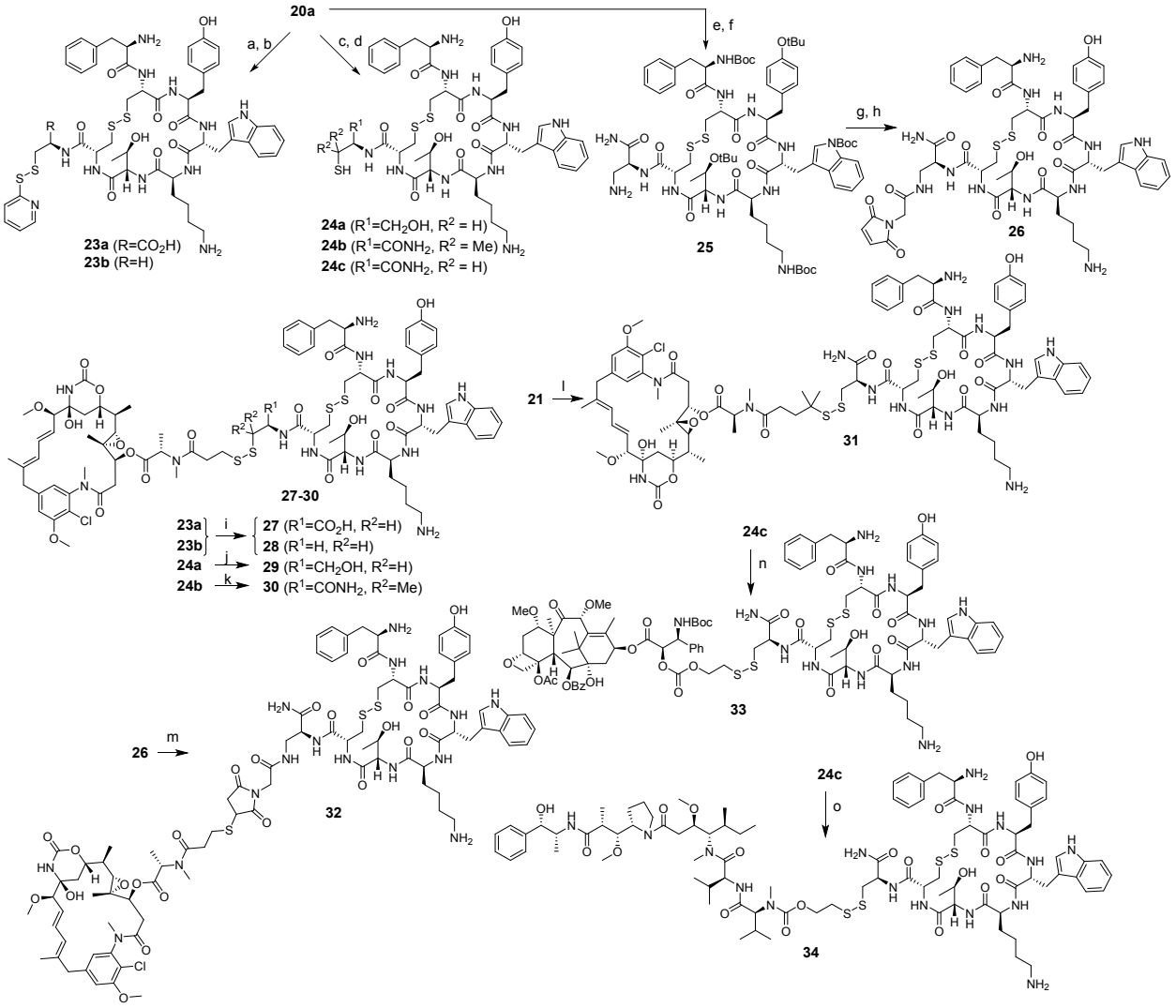

Reagents and conditions: a) HATU, CH_2Cl_2, TrtS-CH_2-CH(R)-NH_2; b) 2,2'-dithiodipyridine, 1,1,3,3-tetramethyldisiloxane, trifluoroethanol, 12N HCl; c) HATU, CH_2Cl_2, TrtS-CR^2_2-CH(R^1)-NH_2 iPr_2NEt; d) TFA, thioanisole, water, triisopropylsilane; e) Dap(Dde)-NH_2, HATU, CH_2Cl_2, iPr_2NEt; f) hydrazine, DMF; g) maleimidoacetic acid, HATU, CH_2Cl_2; h) 92.5:2.5:2.5:2.5 TFA:thioanisole: water:triisopropylsilane; i) DM1, DMF, pH 4.6 acetate buffer; j) **1**, DMF, pH 4.6 acetate buffer; k) **1**, DMF, pH 7.4 phosphate buffer; l) DM4, DMF, pH 7.4 phosphate buffer; m) DM1, DMF, 0.2M NaOAc; n) **2**, DMF, pH 5.6 acetate buffer; o) **3**, DMF, pH 5.6 acetate buffer

Additional SSTR2-targeting conjugates linked at the C-terminal side chain were synthesized as shown in Scheme 4. Modification of the C-terminal amino acid and appending DM1 resulted in conjugates **27**-**30**. Additional payloads were also appended onto the C-terminal side chain; conjugation of DM4[17], cabazitaxel, or MMAE resulted in conjugates **31**, **33**, and **34** respectively. In addition, conjugation of DM1 through a maleimide resulted in conjugate non-cleavable conjugate **32**. Finally, a non-binding control conjugate **37** was synthesized (Scheme 5).

Scheme 5. Synthesis of non-binding control

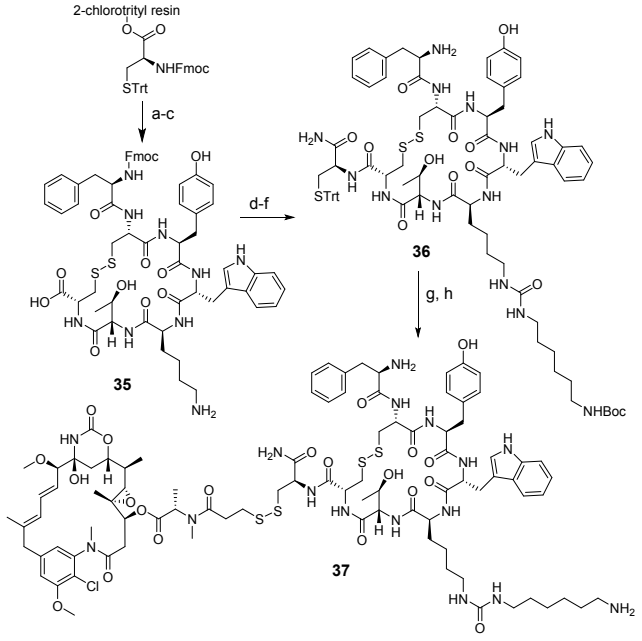

Reagents and conditions: a) iterative SPPS with: Fmoc-threonine(tBu), Nα-Fmoc-Nε-Boc lysine, Nα-Fmoc-N^{in}-Boc-D-tryptophan, Fmoc-tyrosine(tBu), Fmoc-S-trityl-cysteine,

Fmoc-D-phenylalanine; b) 92.5:2.5:2.5:2.5 TFA:thioanisole:water: triisopropylsilane; c) I_2, CH_3CN/water; d) N-Boc-N'-(4-nitrophenylcarbamate)-1,6-hexanediamine, THF, iPr_2NEt, DMAP, 50 °C; e) S-trityl cysteine amide, DMF, HATU, iPr_2NEt; f) piperidine, DMF; g) TFA, triisopropylsilane; h) **1**, DMF, pH 7.4 phosphate buffer

Biological data. Each conjugate was evaluated for SSTR2 affinity by displacement of [I^{125}]Tyr^{11}-SST14 from isolated membrane fractions of SSTR2-expressing CHO-K1 cells. In addition, in vitro cytotoxicity of the octreotide conjugates was assessed in SSTR2-expressing NCI-H524 cells. Each conjugate was incubated with NCI-H524 cells for 2 h either alone or in the presence of 100 μM octreotide, followed by washout and a further 70 h incubation; a typical in vitro experiment is shown in Figure 1. Incubations in the presence of octreotide were performed to fully occupy cell-surface SSTR2 and prevent receptor-mediated uptake of the conjugate. A shift in potency under receptor blockade, compared with conjugate alone, was considered crucial in demonstrating that the cytotoxic effects of the conjugate are dependent on receptor binding and internalization. In vitro data for compounds **7-12**, **14**, **17**, **19**, and **22** is shown in Table 1.

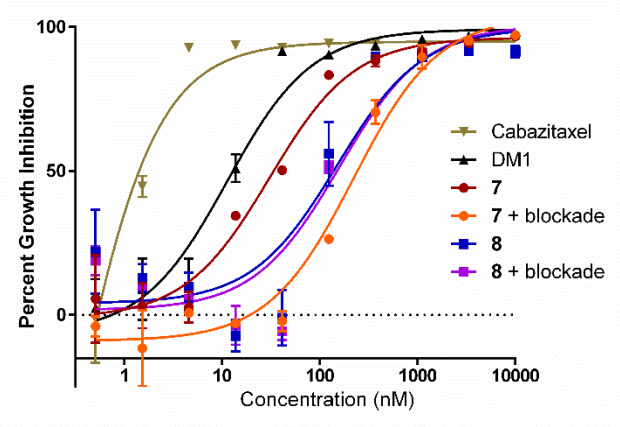

Figure 1. Payload and conjugate cytotoxicity of **7** and **8** in NCI-H524 cells with and without receptor blockade, plus their respective payloads

Table 1. SSTR2 binding data and H524 cell assay data for **7-12**, **14**, **17**, **19**, **22**, payloads, and SST14

Compound	Structure[a]	SSTR2 Ki (pM)[b]	H524 IC50 (nM)[b]	H524 IC50 w/ blockade (nM)[b]
7	DM1-S$(CH_2)_3$-DPhe-[Cys-Phe-DTrp-Lys-Thr-Cys]-Thr-ol	120	30	221
8	MMAE-$CO_2(CH_2)_2SS(CH_2)_3$-DPhe-[Cys-Phe-DTrp-Lys-Thr-Cys]-Thr-ol	770	150	157
9	cabazitaxel-$CO_2(CH_2)_2SS(CH_2)_3$-DPhe-[Cys-Phe-DTrp-Lys-Thr-Cys]-Thr-ol	260	1473	560
10	DM1-Mal-GLFG-MC-S$(CH_2)_3$-DPhe-[Cys-Phe-DTrp-Lys-Thr-Cys]-Thr-ol	140	75	202
11	DM1-S$(CH_2)_3$-DPhe-[Cys-Tyr-DTrp-Lys-Val-Cys]-Trp-NH_2	190	22	115
12	DM1-S$(CH_2)_3$-DPhe-[Cys-Tyr-DTrp-Lys-Thr-Cys]-Thr-OH	15	19	757
14	DM1-S$(CH_2)_2$CO-[NMeLys-Tyr-DTrp-Lys-Thr-Phe]	100	60	865
17	DTyr(CH_2CH_2SDM1)-[Cys-Tyr-DTrp-Lys-Thr-Cys]-Thr-OH	15	15	198
19	DPhe-[Cys-Tyr-DTrp-Lys-Thr-Cys]-Thr-$NHCH_2CH_2$S-DM1	120	44	528
22	DPhe-[Cys-Tyr-DTrp-Lys-Thr-Cys]-Cys(DM1)-NH_2	22	10	910
DM1		n/a	11	n/a
MMAE		n/a	3.7	n/a
cabazitaxel		n/a	0.26	n/a

SST14	5	n/a	n/a

[a] Brackets indicate peptide cyclization. Parentheses after amino acids indicate side chain substitution. Mal = 3-aminopropylmaleimide, MC = maleimidocaproyl. [b] All values determined in duplicate. n/a = not applicable

The performance of these conjugates that utilize octreotide as the targeting ligand was noticeably affected by the payload; while DM1 conjugate **7** showed potency near that of payload alone, the potency of both cabazitaxel conjugate **8** and MMAE conjugate **9** were several orders of magnitude worse than their respective payloads. Additionally, only **7** exhibited any signs of receptor-dependent cytotoxicity. The receptor affinity was also clearly affected by the payload, as both **8** and **9** had lower affinity for SSTR2 than DM1 conjugate **7**. While replacement of the disulfide linker with a protease-cleavable linker (**10**) did not significantly change the receptor affinity, it was less potent in the NCI-H524 cellular assay, indicating that disulfide linkers might be optimal for release upon SSTR2-mediated internalization.

While conjugate **7** demonstrated initial signs of receptor-dependent cytotoxicity, the receptor affinity was significantly worse than native ligand SST14. Given that conjugates may have to compete against endogenous somatostatin for uptake in SSTR2-expressing

cells, and the knowledge that tumor uptake of small molecule drug conjugates is predicted to track with receptor affinity[8], it was important to examine alternative SSTR2 targeting ligands in order to improve receptor affinity. The Tyr[3]-octreotate targeting ligand of conjugate **12** clearly provided superior receptor affinity compared to octreotide conjugate **7**, following the pattern observed with radiolabeled conjugates[24]. Conjugate **12** also provided the largest window between cellular potency of the conjugate and potency under receptor blockade. Vapreotide conjugate **11** appeared nearly as potent in the cellular assay, but this potency did not shift nearly as much under receptor blockade, indicating that some of the cellular potency may come from either passive permeability of the more lipophilic ligand, or conjugate instability and extracellular release of the payload under the assay conditions. Cyclic 6-mer targeting ligand conjugate **14** did not demonstrate any noticeable advantages to octreotide conjugate **7** in terms of in vitro properties.

Examination Tyr[3]-octreotate conjugates linked to DM1 at sites other than the N-terminus show that substitution at either the N-terminal side chain (**17**) or C-terminal side chain (**22**) maintained receptor affinity and cellular potency compared to N-terminal conjugate **12**. Only C-terminal conjugate **19** showed inferior receptor affinity and cellular

potency among Tyr^3-octreotate/DM1 conjugates. In order to differentiate these conjugates, several compounds evaluated in vivo for their ability to target DM1 to SSTR2-expressing NCI-H69 tumors. Selected conjugates were administered to NCI-H69 tumor-bearing mice at 1 mg/kg i.v., while unconjugated DM1 was dosed as a control at 0.4 mg/kg. At 24 h, tumors were excised and treated with excess tris-2-carboxyethylphosphine (TCEP) to reduce any disulfide bonds. The resulting free thiols trapped with N-ethyl maleimide (NEM), and total DM1-NEM adduct levels measured. Values normalized for total DM1 dose are presented in Figure **2**. Conjugates **7**, **11**, and **19**, each with SSTR2 affinity >100 pM, exhibited equal, or only slightly superior, DM1 tumor accumulation compared with untargeted DM1. Tyr^3-octreotate conjugates **12**, **17**, and **22** were superior to other targeting ligand DM1 conjugates. Importantly, conjugate **22** demonstrated the greatest ability to deliver DM1 to an SSTR2-expressing tumor.

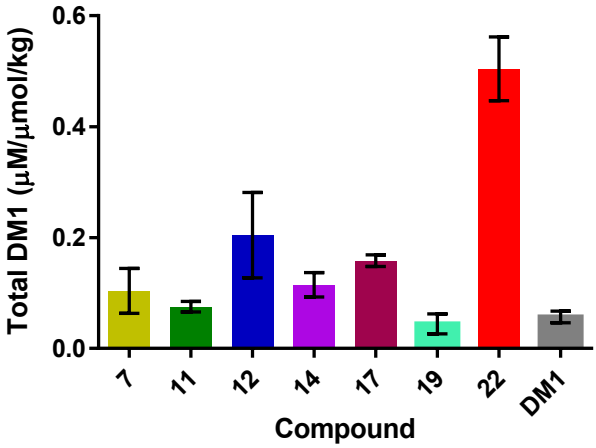

Figure 2. Dose-normalized DM1 levels in NCI-H69 tumors 24 h after conjugate dosing

Table 2. In vitro data for compounds **22**, **27-34**

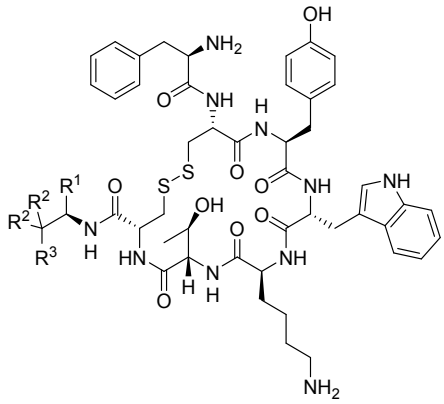

Compound	R^1	R^2	R^3	SSTR2 Ki (pM)[b]	H524 IC50 (nM)[b]	H524 IC50 w/ blockade (nM)[b]
22	$CONH_2$	H	S-DM1	22	10	910
27	CO_2H	H	S-DM1	13	183	1597
28	H	H	S-DM1	61	10	692
29	CH_2OH	H	S-DM1	18	42	1389
30	$CONH_2$	Me	S-DM1	15	8	1041

31	$CONH_2$	H	S-DM4	75	27	581
32	$CONH_2$	H	NH-MalAc-DM1[a]	140	91	2524
33	$CONH_2$	H	$SSCH_2CH_2CO_2$-cabazitaxel	970	7	14
34	$CONH_2$	H	$SSCH_2CH_2CO_2$-MMAE	180	1258	1427

[a] MalAc = maleimidoacetate. [b] All values determined in duplicate.

Additional conjugates with payloads conjugated at the C-terminal side chain are shown in Table 2. Modification of the C-terminal amide of **22** to an acid (**27**) or amino alcohol (**29**) maintained receptor affinity, but noticeably reduced potency in NCI-H524 cells. Complete removal of the C-terminal amide (**28**) maintained cellular potency, but reduced receptor affinity.

Slower releasing hindered disulfides were also examined[25]. Appending a gem-dimethyl group on the payload side by using DM4[17] rather than DM1 (**31**) resulted in reduced cellular potency and receptor affinity. However, placing the gem-dimethyl group on the ligand side of the disulfide bond by utilizing penicillamine as the linking amino acid rather than cysteine (**30**) showed similar in vitro properties to **22**. Non-cleavable DM1 conjugate **32** does demonstrate receptor-dependent cytotoxicity, showing that release of free

payload is not strictly necessary for toxicity, however conjugate **32** was significantly less potent than disulfide-linked conjugates **22** and **30**.

We investigated if the C-terminal side chain conjugation site of **22** was amenable to delivery of other microtubule agent payloads. Analogs of **22** where the payload has been replaced by either cabazitaxel (**33**) or MMAE (**34**) shows that the in vitro properties of conjugates linked at the C-terminal side chain are payload-dependent. The SSTR2 binding affinity of both **33** and **34** were dramatically reduced compared to **22**, and neither exhibited much receptor dependent cytotoxicity. To evaluate if this reduced binding affinity obtained with other payloads had functional consequences for SSTR2 activity, we examined **22** and **33** in an SSTR2 internalization assay (DiscoverX) (Figure 3). While DM1 conjugate **22** is more efficacious than native ligand SST28 at inducing receptor internalization, the cabazitaxel conjugate **33** was much less potent at inducing receptor internalization, demonstrating that the inferior receptor affinity of **33** also leads to reduced SSTR2 agonist activity. Thus, while the C-terminal side chain of Tyr^3-octreotate appears to be an excellent site for DM1 conjugation, the effectiveness of this conjugation site does not translate for other payloads.

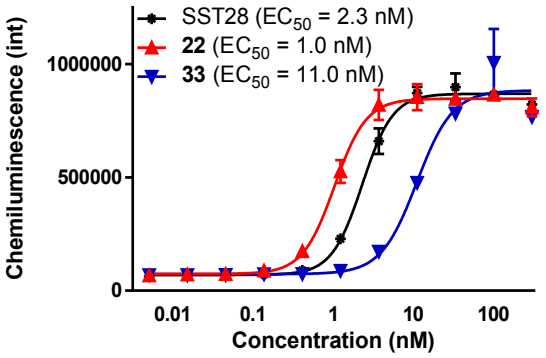

Figure 3. SSTR2 internalization by **22**, **33**, and SST28

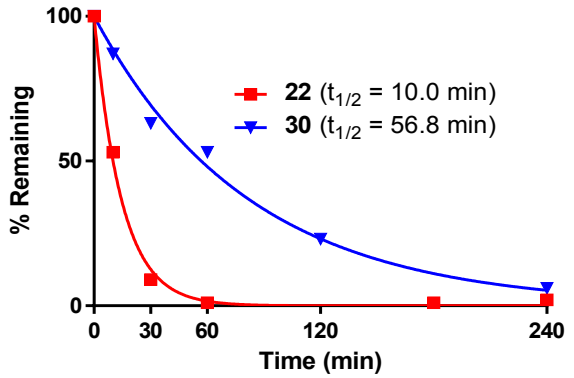

Figure 4. Stability of **22** and **30** in 5 mM GSH at 37 °C

In order to further explore the importance of the release rate of the disulfide linker, **22** and **30** were examined in several additional in vitro and in vivo studies. Stability experiment of both compounds in 5 mM GSH (Figure 4) demonstrating that **30** possessed better stability to reducing conditions. However, side-by-side comparisons of both **22** and **30** in beagle dog (Figure 5) shows that the increased stability of the linker does not

dramatically affect pharmacokinetics. While **30** had a modestly higher AUC (Table 3), this change is only 1.6-fold, suggesting that the stability of the linker is not the major metabolic liability of **22**. In an SSTR2-expressing NCI-H69 mouse xenograft (Figure 6), both **22** and **30** were able to induce complete regressions at 2.0 mg/kg i.v. without any body weight loss (see supporting information); however, **22** was more potent at 1.3 mg/kg. Thus, the improved stability of **30**, and its modestly better plasma pharmacokinetics, did not translate into greater efficacy.

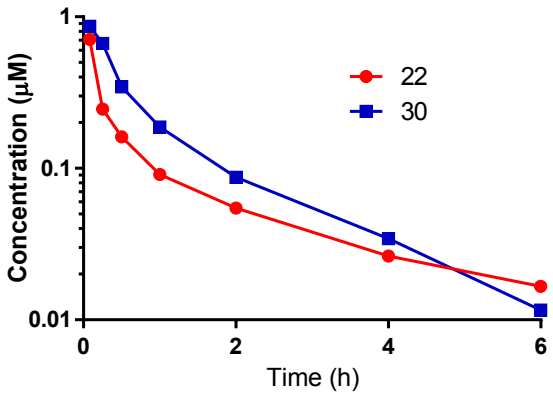

Figure 5. Beagle dog pharmacokinetics (n=1) of 0.1 mg/kg **22** and **30** i.v.

Table 3. Select beagle dog PK parameters

Parameter	22	30
$t_{1/2}$ (h)	2.33	1.38
Cmax (µmol/L)	0.708	0.867
AUC 0-6h (µmol/L*h)	0.470	0.769

Cl (mL/kg/min)	1.66	1.09

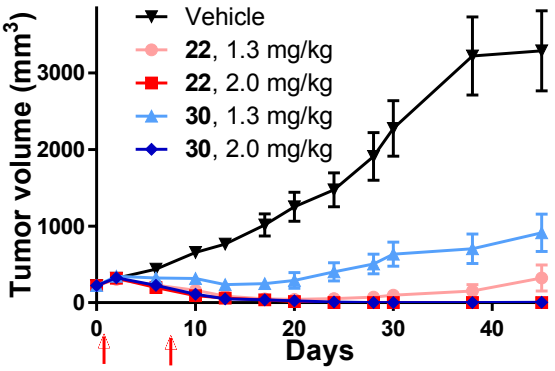

Figure 6. **22** and **30** in NCI-H69 xenograft efficacy. Arrows indicate dosing days.

In order to demonstrate in vivo receptor dependence of **22**, it was compared with conjugate **37**, which is structurally similar but with the lysine residue of the SSTR2 binding pharmacophore capped with a 1,6-hexanediamine urea. This particular capping group was selected in order to keep the overall charge and lipophilicity of **37** similar to that of **22**. However, this modification of the lysine residue almost completely abolished SSTR2 binding as well as receptor-dependent cytotoxicity (Table **4**). Conjugate **37** (0.7 mg/kg i.v.) was not efficacious in an NCI-H69 xenograft model (Figure **7**).

Table 4. SSTR2 binding data and H524 cell assay data of **22** and its non-binding control **37**

Compound	SSTR2 K_i	H524 IC_{50} (nM)	H524 IC_{50} w/ blockade (nM)
22	22 pM	10	910
37	3.35 μM	581	644

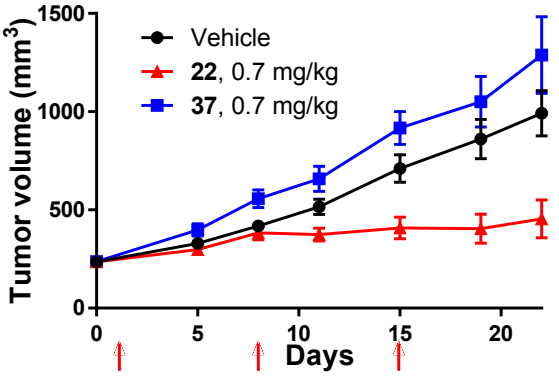

Figure 7. 22 and **37** in NCI-H69 xenograft efficacy. Arrows indicate dosing days.

Conjugate **22** was tested for binding against all five somatostatin receptor isoforms, indicating good selectivity for SSTR2 (Table **5**). While binding to SSTR2 is close to that of the native ligand SST14, SSTR5 binding is 30-fold lower than the native ligand, and binding to all other isoforms is >600-fold lower than the native ligand. In addition, **22** was examined for selectivity against other GPCRs; **22** was evaluated against a panel of 119 GPCRs, examining for both agonist and antagonist activity. Conjugate **22** was inactive against all GPCRs in this panel except for SSTR2 and SSTR5 (see supporting

information). In addition, the passive permeability of **22** was extremely low (Caco-2 A-B P_{app} = 0.018x10^{-6} cm/s), indicating that entry of **22** into non-SSTR2 expressing cells, either through other receptors or passive diffusion, would be minimal. The activity of **22** was also examined in other SSTR2-positive xenografts. Conjugate **22** demonstrated complete regressions in HCC-33 small cell lung carcinoma xenografts at 1.0 mg/kg i.v., and IMR-32 neuroblastoma xenografts at 1.5 mg/kg i.v. (Figure 8).

Table 5. SSTR2 selectivity of **22**

	SSTR1 K_d	SSTR2 K_d	SSTR3 K_d	SSTR4 K_d	SSTR5 K_d
22	310 nM	16 pM	19.8 nM	5.48 μM	9.6 nM
SST14	290 pM	5 pM	32 pM	200 pM	320 pM

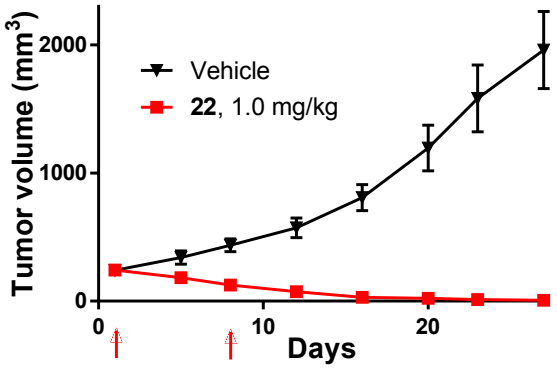

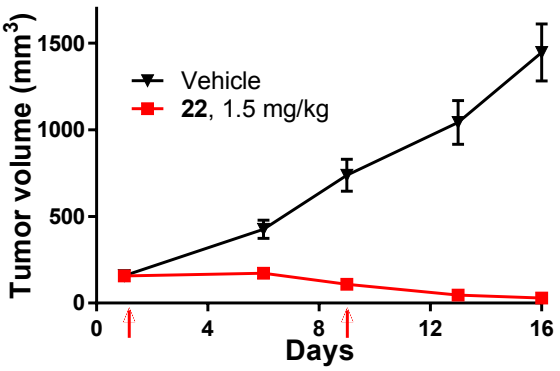

Figure 8. **22** in HCC-33 (top) and IMR-32 (bottom) xenografts. Arrows indicate dosing days.

Conclusion

In summary, we have examined several SSTR2 agonist ligands, conjugation sites, and microtubule agent payloads for their ability to target payloads to SSTR2-expressing cells. Optimization for receptor affinity anerd receptor-dependent cellular potency have led to the discovery PEN-221 (**22**), a novel maytansinoid-containing conjugated targeted to SSTR2. Uniquely among SSTR2-targeting peptide conjugates, the payload of **22** is conjugated at the C-terminal side chain, which allows for good receptor affinity and excellent levels of DM1 delivered into SSTR2-expressing tumors. Conjugate **22** has excellent affinity for SSTR2, is very potent at inducing receptor internalization, and has

good selectivity for SSTR2 over other somatostatin receptor subtypes as well as other GPCRs. PEN-221 (**22**) is able to induce regressions in several SSTR2-expressing xenograft models, and is currently being evaluated in human clinical trials.

Experimental section

Chemistry general methods. DM1, DM4, and MMAE were purchased from Ontario Chemicals, cabazitaxel was purchased from Indena, octreotide and vapreotide were purchased from ChemPep, Tyr^3-octreotate was synthesized at ChemPartner, and all other reagents were purchased from Chem-Impex, Aldrich, Fisher, or Ark Pharm, and used without further purification. Solid phase peptide synthesis was carried out on a CEM Liberty Blue peptide synthesizer. All silica gel chromatography was carried out on RediSep Rf Gold silica gel disposable flask columns (20-40 micron) on a Teledyne Isco combiflash system. Reverse phase chromatography was carried out on RediSep Rf Gold C18 reverse phase columns (20-40 micron), and preparative HPLC purification was done on a Waters Sunfire C18 OBD Prep HPLC column, 100 Å, 5 μm, 30 x 150 mm. Final compounds were lyophilized on an SP Scientific Benchtop Pro 9 EL lyophilizer. Chemical purities were >95% for all final compounds, as assessed by an Agilent 1100 LCMS with

an Agilent Eclipse Plus C18 column, 3.5 μm, 4.6 x 100 mM, with detection at 254 and 280 nm. Mass spectrometry data were gathered on an Agilent G1946D mass spectrometer with electrospray ionization. Procedures for synthesis of compounds **1-19**, and **23-37** are in the supporting information.

Radioligand binding assays. Radioligand binding assays were performed at Eurofins Discovery Services, Taipei. CHO-K1 cells stably transfected with a plasmid encoding the desired human somatostatin receptor were used to prepare membranes in modified HEPES pH 7.4 buffer using standard techniques. An aliquot (1 μg for SSTR1, 0.1 μg for SSTR2, 0.375 μg for SSTR3, 0.25 μg for SSTR4, 2 μg for SSTR5) of membrane was incubated with 0.03 nM (SSTR2) or 0.1 nM (all other SSTRs) [^{125}I]somatostatin for either 240 minutes (SSTR2) or 120 minutes (all other SSTRs) at 25 °C. Non-specific binding was estimated in the presence of 1 μM somatostatin. Membranes were filtered and washed 3 times and the filters counted to determine [^{125}I]somatostatin specifically bound. Compound treatment was done at six concentrations, with 10 nM as highest concentration and five-fold dilutions for SSTR2, 10 μM and 3-fold dilutions for SSTR1 and SSTR4, or 1 μM and 10-fold dilutions for SSTR3 and SSTR5.

Cytotoxicity assay. NCI-H524 (ATCC) human lung cancer cells were plated in 96 well, V-bottomed plates (Costar) at a concentration of 5,000 cells/well and 24 hours later were treated with compound for 2 hours. Compound starting dose was 10 μM and three-fold serial dilutions were done for a total of ten points. For experiments with octreotide competition, cells were first treated with 100 μM octreotide acetate (Chempep) for 30 min, then treated with compound as above. After 2 hr compound treatment, cells were spun down, the drug containing media was removed and fresh complete medium was added and used to resuspend the cells, which were spun again. After removal of the wash media, the cells were resuspended in complete medium, then transferred into white walled, flat bottomed 96 well plates. Cells were further incubated for an additional 70 hours to measure inhibition of cell proliferation. Proliferation was measured using Cell Titer Glo reagent using the standard protocol (Promega) and a Glomax multi + detection system (Promega). Percent proliferation inhibition was calculated using the following formula: % inhibition = (control-treatment)/control*100. Control is defined as vehicle alone. IC50 curves were generated using the nonlinear regression analysis (four parameter) with GraphPad Prism 6.

Xenograft studies. All studies were conducted in accordance with the Tarveda Therapeutics Institutional Animal Care and Use Committee (IACUC). All mice were treated in accordance with the OLAW Public Health Service Policy on Human Care and Use of Laboratory Animals and the ILAR Guide for the Care and Use of Laboratory Animals. To establish a subcutaneous xenograft model, NCI-H69 (ATCC) human small cell lung cancer cells or HCC-33 (ATCC) human small cell lung cancer cells were cultured in RPMI 1640 medium containing 10% fetal bovine serum, or IMR32 (ATCC) neuroblastoma cancer cells were cultured in Eagle's minimum essential medium containing 10% fetal bovine serum. The cells were cultured in tissue culture flasks in a humidified incubator at 37°C, in an atmosphere of 5% CO2 and 95% air. Cells were harvested, centrifuged and resuspended in media and Matrigel (1:1 ratio) at a concentration of 2.5×10^7 cells/mL. Female athymic nude mice (CrTac:NCr-Foxn1nu, Taconic) were implanted subcutaneously in the right flank with 2.5×10^6 cells (NCI-H69, HCC-33) or 1×10^7 cells (IMR-32). When tumors reached a volume of 150-250 mm^3 mice were randomized into groups of 10 with similar mean tumor size. Compounds were formulated at the desired dose in 10% propylene glycol in 5 mM citrate buffer (pH=4) for

NCI-H69 xenografts, or 0.1% Solutol HS 15/5% mannitol/WFI for HCC33 and IMR32 xenografts. Mice received intravenous injection of compound into the tail vein on days indicated. Tumor volume was measured in two dimensions using calipers and volume was calculated using the formula: $(w^2 \times l)/2 = mm^3$. The results were plotted as mean tumor volume ± SEM of each group over time.

DM1 analysis in NCI-H69 tumors. NCI-H69 tumors were established as above. When tumors reached a volume of 250-600 mm^3, mice were randomized into groups of 3. Compounds were formulated in either 10% propylene glycol in WFI (DM1) or 10% propylene glycol in 5 mM citrate buffer pH=4 (all others). 24 h after dosing, tumors were excised, weighed, and 0.1 M of ammonium bicarbonate buffer pH 8.0 (Fisher Scientific) was added to the tumors at the ratio of 1:4 (w/v). Samples were kept on ice and homogenized for 20-30 sec each or until no intact tissue was observed. DM1 stock solution in methanol (Fisher Scientific) was used to prepare standards and assay controls in the blank NCI-H69 tumor homogenate.

For analysis, a 100 µL of the tumor homogenate sample was added onto a 96-well plate followed by the 10 µL addition of the 0.5 M Tris[2-carboxyethyl]phosphine, TCEP, (Sigma

Aldrich) and 400 µL of acetonitrile (Fisher Scientific). The plate was capped, mixed, and incubated on an orbital shaker for 15 min at 37°C. Then 50 µL of 0.2 M N-ethylmaleimide, NEM (Sigma Aldrich) was added and the plate was incubated at 37°C on an orbital shaker for another 15 min. After the incubation, 10 µL of internal standard was added and the plate was centrifuged for 5 min at 3700 x g. Clear supernatant was transferred to a new plate for LC-MS/MS analysis.

SSTR2 internalization. The PathHunter® eXpress SSTR2 Activated GPCR Internalization Assay from DiscoverX was used to measure SSTR2 internalization. Cells were plated according to the manufacture's protocol and incubated for 24 hours. After 24 hours, compounds were added at a starting concentration of 300nM, which was then diluted 3-fold for 11 data points. Compounds and cells were then incubated for 4 hours. Detection reagent was then added according to the manufactures protocol and incubated for 60 minutes at room temperature, after which the chemiluminescent signal was measured.

GSH stability. A 5 mM solution of GSH was made in PBS, and 990 µL aliquots dispensed into Eppendorf tubes. To each tube was added 10 µL of a stock solution of

either **22** or **30** (1 mM in MeOH), and the solutions incubated at 37°C. At 30 min, 1 h, 2 h, 4 h, and 6 h, 100 μL of GSH solution was added to 600 μL of 500 μM N-ethyl maleimide solution in 1% ethanol, and the samples analyzed for parent conjugate by LCMS/MS.

Boc-DPhe-cyclo[Cys-Tyr(tBu)-DTrp(Boc)-Lys(Boc)-Thr(tBu)-Cys]-OH (**20a**). Fmoc-cystine(Trt)-OH was loaded onto 2-chlorotrityl resin (30.0 g, 0.739 mmol/g loading). Iterative deprotection with 4:1 DMF:piperidine and coupling subsequently with Fmoc-threonine(tBu), Nα-Fmoc-Nε-Boc-lysine, Nα-Fmoc-N^{in}-Boc-D-tryptophan, Fmoc-tyrosine(tBu), Fmoc-cysteine(Trt), and Boc-D-phenylalanine gave 90.2 g of the protected linear peptide (60.2 g total peptide loaded, 0.369 mmol/g loading of final protected resin). A portion of this linear peptide (10.0 g, 3.69 mmol) was taken, and DMF (25 mL) and pyridine (1.16 g, 14.7 mmol) were added. A solution of iodine (1.87 g, 7.36 mmol) in DMF (25 mL) was added, and the resin stirred for 20 minutes at room temperature. The resin was drained, washed with DMF (25 mL), and additional DMF (25 mL) and pyridine (1.16 g, 14.7 mmol) were added. A solution of iodine (1.87 g, 7.36 mmol) in DMF (25 mL) was added, the resin stirred for 20 minutes at room temperature. The resin was drained, washed with DMF (2 x 25 mL) and dichloromethane (4 x 20 mL). The resin was then

treated with 4:1 dichloromethane:hexafluoroisopropanol (60 mL) for 1 h. The dichloromethane: hexafluoroisopropanol solution was collected, the resin washed with dichloromethane (25 mL), and treated again with 4:1 dichloromethane:hexafluoroisopropanol (60 mL) for 1 h. The dichloromethane: hexafluoroisopropanol solution was collected, the resin washed with dichloromethane (25 mL), and the combined dichloromethane:HFIP solutions, and dichloromethane washings, were dried in vacuo. The remaining solid was loaded onto an 80 g silica gel column. Elution with 0% to 10% methanol in dichloromethane provided **20a** (2.97 g, 2.18 mmol, 59% yield). ^{1}H NMR (400 MHz, CD_3OD) δ 8.11 (d, J = 8.4 Hz, 1H), δ 7.98 (s, 1H), δ 7.55 (d, J = 8 Hz, 1H), δ 7.49 (br s, 1H), δ 7.24-7.21 (m, 8H), δ 7.08 (d, J = 7.2 Hz, 2H), δ 6.84 (d, J = 8 Hz, 2H), δ 4.99-4.90 (m, 2H), δ 4.64 (t, J = 6.8 Hz, 1H), δ 4.49-4.40 (m, 2H), δ 4.15 (t, J = 4.8 Hz, 1H), δ 4.06 (dd, J = 13.2, 2.8 Hz, 1H), δ 3.20-3.01 (m, 3H), δ 3.01-2.90 (m, 5H), δ 2.90-2.78 (m, 5H), δ 1.66 (s, 9H), δ 1.41 (s, 9H), δ 1.36 (s, 9H), δ 1.28 (s, 9H), δ 1.26 (s, 9H), δ 1.25-1.18 (m, tH), δ 0.70 (br s, 2H).

Boc-DPhe-cyclo[Cys-Tyr(tBu)-DTrp(Boc)-Lys(Boc)-Thr(tBu)-Cys]-Cys(Trt)-NH_2 (**20b**). A flask was charged with **20a** (19.0 g, 14.0 mmol), S-trityl L-cysteine amide (5.57 g, 15.6

mmol) and HATU (5.84 g, 15.4 mmol). Dichloromethane (190 mL) was added, followed by diisopropylethylamine (4.88 mL, 27.9 mmol). The reaction was stirred at room temperature for 3 hours, then loaded directly onto a 330 g silica gel column. Elution with 0% to 10% methanol in dichloromethane provided **20b** (23.8 g, 13.9 mmol, 99% yield). ^{1}H NMR (400 MHz, CD_3OD) δ 8.12 (d, J = 8.4 Hz, 1H), δ 7.51 (d, J = 7.6 Hz, 1H), δ 7.44 (s, 1H), δ 7.38-7.30 (m, 9H), δ 7.28-7.15 (m, 13H), δ 7.09 (d, J = 7.6 Hz, 1H), δ 6.87 (d, J = 8.4 Hz, 2H), δ 5.59-5.40 (m, 2H), δ 4.68 (d, J = 3.6 Hz, 1H), δ 4.57 (dd, J = 10, 5.2 Hz, 1H), δ 4.49 (dd, J = 10.4, 5.2 Hz, 1H), δ 5.36-4.29 (m, 2H), δ 4.11 (dd, J = 10.4, 3.2 Hz, 1H), δ 3.97 (dt, J = 10, 3.6 Hz, 1H), δ 3.22 (dd, J = 11.6, 4 Hz, 1H), δ 3.11-3.00 (m, 5H), δ 2.96-2.58 (m, 14H), δ 1.67 (s, 9H), δ 1.42 (s, 9H), δ 1.29 (s, 9H), δ 1.27-1.24 (m, 8H), δ 1.17 (s, 9H), δ 1.07 (d, J = 6.4 Hz, 3H), δ 0.55 (br s, 2H).

DPhe-cyclo[Cys-Tyr-DTrp-Lys-Thr-Cys]-Cys(SPy)-NH_2 (**21**). A flask was charged with **20b** (3.77 g, 2.03 mmol) and 2,2'-dithiodipyridine (536 mg, 2.43 mmol). Trifluoroethanol (19 mL) was added, the mixture sonicated until everything went into solution (~5 minutes). 1,1,3,3-tetramethyldisiloxane (0.715 mL, 4.05 mmol) was added, followed by 12N aqueous HCl (3.8 mL). The reaction was stirred at room temperature for 1 h, after which

acetonitrile (38 mL) was added. The resulting suspension was stirred for 30 minutes, then filtered and the remaining solid washed with additional acetonitrile (30 mL). The remaining solid was dissolved in 1M aqueous acetic acid (100 mL). The solution was stirred for 2 hours, then loaded directly onto a 275 g C18 Aq Isco column. The column was flushed with 150 mL aqueous 100 mM ammonium acetate, followed by 300 mL water with 0.1% acetic acid. A gradient of 0% to 45% acetonitrile in water with 0.1% acetic acid was then run, and the product-containing fractions pooled, approximately half the volume removed under vacuum, and the remaining material frozen and lyophilized to give **21** as the acetate salt (2.04 g, 1.58 mmol, 77% yield). ^{1}H NMR (500 MHz, CD_3OD) δ 8.42 (d, J = 9.5 Hz, 1H), δ 7.83-7.78 (m, 2H), δ 7.45 (d, J = 8 Hz, 1H), δ 7.33-7.27 (m, 6H), δ 7.23-7.21 (m, 2H), δ 7.09-7.06 (m, 3H), δ 7.01-6.99 (m, 2H), δ 6.76 (d, J = 6.5 Hz, 2H), δ 5.09-5.02 (m, 3H), δ 4.64-4.61 (m, 2H), δ 4.39 (q, J = 3 Hz, 1H), δ 4.13 (dd, J = 11.5, 5 Hz, 1H), δ 3.96 (dd, J = 11, 4 Hz, 1H), δ 3.74 (dd, J = 8, 6.5 Hz, 1H), δ 3.25 (dd, J = 13.5, 9.5 Hz, 1H), δ 3.12-3.01 (m, 4H), δ 2.94-2.82 (m, 6H), δ 2.62-2.58 (m, 2H), δ 1.92 (s, acetate), δ 1.69 (br s, 1H), δ 1.34-1.22 (m, 6H), δ 0.52 (br s, 2H). ESI MS (+) (*m/z*): Calcd for $C_{53}H_{66}N_{12}O_{10}S_4$ = 1158.4, found = 1159.4 (M+1).

DPhe-cyclo[Cys-Tyr-DTrp-Lys-Thr-Cys]-Cys(DM1)-NH_2 (PEN-221, 22). A flask was charged with **21** acetate salt (645 mg, 0.461 mmol), and this was dissolved in a mixture of THF (10 mL), and pH 3.7 acetate buffer (10 mL, made from mixing 9.0 mL 0.2M AcOH and 1.0 ml 0.2M NaOAc). To this was then added a solution of DM1 (359 mg, 0.470 mmol) in THF (10 mL). The reaction was stirred at room temperature for 1 h, and the reaction mixture concentrated under vacuum at 35 °C at 10 mbar for 45 min to remove the THF. DMF (3 mL) and 1% aqueous acetic acid (9 mL) were added, and the reaction mixture loaded onto a 100 g C18 Aq Isco gold column. Elution with a gradient of 5% to 40% acetonitrile in water with 0.1% AcOH provided **22** as the acetate salt (777 mg, 0.408 mmol, 86% yield). ^{1}H NMR (400 MHz, CD_3OD) δ 7.42 (d, J = 7.6 Hz, 1H), δ 7.35-7.23 (m, 6H), δ 7.10-7.02 (m, 6H), δ 6.76 (d, J = 8 Hz, 2H), δ 6.67 (d, J = 11.2 Hz, 1H), δ 6.64 (s, 1H), δ 6.57 (dd, J = 14.4, 11.6 Hz, 1H), δ 5.70 (dd, J = 15.6, 8.8 Hz, 1H), δ 5.45 (q, J = 7.2 Hz, 1H), δ 4.99-4.96 (m, 2H), δ 4.68-4.59 (m, 3H), δ 4.41-4.38 (m, 2H), δ 4.18 (td, J = 10, 5.2 Hz, 1H), δ 4.07 (dd, J = 10.8, 4.8 Hz, 1H), δ 3.92 (s, 3H), δ 3.88 (dd, J = 8.8, 2.4 Hz, 1H), δ 3.79 (t, J = 6.8 Hz, 1H), δ 3.64 (d, J = 12.4 Hz, 1H), δ 3.55 (d, J = 9.2 Hz, 1H), δ 3.33 (s, 3H), δ 3.20 (d, J = 13.2 Hz, 1H), δ 3.16 (s, 3H), δ 3.11-3.06 (m, 2H), δ 3.03-2.86

(m, 9H), δ 2.85 (s, 3H), δ 2.84-2.77 (m, 3H), δ 2.66 (d, J = 14 Hz, 1H), δ 2.59 (t, J = 8 Hz, 2H), δ 2.12 (dd, J = 14.4, 2 Hz, 1H), δ 1.94 (s, acetate), δ 1.66 (s, 3H), δ 1.64-1.47 (m, 4H), δ 1.30 (d, J = 6.8 Hz, 3H), δ 1.28 (d, J = 6 Hz, 3H), δ 1.27-1.23 (m, 3H), δ 1.22 (d, J = 6.8 Hz, 3H), δ 0.83 (s, 3H), δ 0.47-0.41 (m, 2H). ^{13}C NMR (125 MHz, CD_3OD) δ 176.19, δ 174.76, δ 173.96, δ 173.18, δ 172.88, δ 172.69, δ 172.28, δ 171.29, δ 169.91, δ 157.61, δ 155.39, δ 143.19, δ 142.90, δ 140.50, δ 138.06, δ 137.05, δ 134.59, δ 131.67, δ 130.72, δ 130.12, δ 129.78, δ 128.84, δ 128.65, δ 126.87, δ 125.15, δ 123.06, δ 122.58, δ 120.29, δ 119.66, δ 119.46, δ 116.40, δ 115.28, δ 112.57, δ 110.37, δ 89.89, δ 81.82, δ 79.55, δ 75.76, δ 68.89, δ 68.21, δ 61.97, δ 61.46, δ 58.34, δ 57.36, δ 57.15, δ 56.44, δ 56.43, δ 56.26, δ 54.15, δ 54.02, δ 53.91, δ 53.61, δ 47.48, δ 45.53, δ 42.19, δ 40.47, δ 40.46, δ 40.37, δ 40.29, δ 39.71, δ 37.97, δ 36.74, δ 34.91, δ 33.56, δ 31.30, δ 28.19, δ 27.60, δ 23.55, δ 20.50, δ 15.83, δ 14.88, δ 13.93, δ 12.73. ESI MS (+) (*m/z*): Calcd for $C_{83}H_{109}ClN_{14}O_{20}S_4$ = 1784.6, found = 893.4 [(M+2H)/2].

Author Information

*Email: bwhite@tarvedatx.com. Phone: (617)-639-1845

Supporting information

Mouse body weights for NCI-H69 xenograft study (Figure 6), synthetic procedures for compounds 1-19, and 23-37, GPCR screening data, and molecular formula strings and biological data (CSV) in Table 1, Table 2, and Table 4 are available in the supporting information.

Abbreviations used

ADC, antibody-drug conjugate; AUC, area under the curve; DCM, dichloromethane; DMAP, 4-dimethylaminopyridine; DMF, dimethylformamide; EDT, 1,2-ethanedithiol; GPCR, G protein coupled receptor; GSH, glutathione; HATU, O-(7-azabenzotriazol-1-yl)-N,N,N′,N′-tetramethyluronium hexafluorophosphate; HOAt, 1-Hydroxy-7-azabenzotriazole; MMAE, monomethyl auristatin E; NEM, N-ethyl maleimide; SPPS, solid phase peptide synthesis; SST, somatostatin; SSTR, somatostatin receptor; TCEP, tris-2-carboxyethylphosphine; TFA, trifluoroacetic acid.

References

Garnock-Jones, K. P. Brentuximab vedotin: A review of its use in patients with Hodgkin lymphoma and systemic anaplastic large cell lymphoma following previous treatment failure. *Drugs*, 2013, *73*, 371-381.

[2] Lambert, J. M.; Chari, R. V. Ado-trastuzumab emtansine (T-DM1): An antibody-drug conjugate (ADC) for HER2-positive breast cancer. *J. Med. Chem.* 2014, *57*, 6949-6964.

[3] Goy, A.; Forero, A.; Wagner-Johnston, N.; Ehmann, W. C.; Tsai, M.; Hatake, K.; Ananthakrishnan, R.; Volkert, A.; Vandendries, E.; Ogura, M. A phase 2 study of inotuzumab ozogamicin in patients with indolent B-cell non-Hodgkin lymphoma refractory to rituximab alone, rituximab and chemotherapy, or radiotherapy. *Br. J. Haematol.* 2016, *174*, 571-581.

[4] Jain, R. K. Transport of molecules, particles, and cells in solid tumors. *Annu. Rev. Biomed. Eng.* 1999, *1*, 241-263.

[5] Baxter, L. T.; Jain, R. K. Transport of fluid and macromolecules in tumors. IV. A microscopic model of the perivascular distribution. *Microvasc. Res.* 1991, *41*, 252-272.

[6] Beckman, R. A.; Weiner, L. M.; Davis, H. M. Antibody constructs in cancer therapy. *Cancer* 2007, *109*, 171-179.

[7] a) Vrettos, E. I.; Mezö, G.; Tzakos, A. G. On the design principles of peptide-drug conjugates for targeted drug delivery to the malignant tumor site. *Beilstein J. Org. Chem.* 2018, *14*, 930-954. b) Vergote, I.; Leamon, C. P. Vintafolide: A novel targeted therapy for the treatment of folate receptor expressing tumors. *Ther. Adv. Med. Oncol.* 2015, *7*, 206-218.

[8] Schmidt, M. M.; Wittrup, K. D. A modeling analysis on the effects of molecular size and binding affinity on tumor targeting. *Mol. Cancer Ther.* 2009, *8*, 2861-2871.

[9] Sheppard, M.; Shapiro, B.; Pimstone, B.; Kronheim, S.; Berelowitz, M. Gregory, M. Metabolic clearance and plasma half-disappearance time exogenous somatostatin in man. *Journal of Clinical Endocrinology & Metabolism* 1979, *48*, 50-53.

[0] Hannon, J. P.; Nunn, C.; Stolz, B.; Bruns, C.; Weckbecker, G.; Lewis, I.; Troxler, T.; Hurth, K.; Hoyer, D. Drug design at peptide receptors. *J. Mol. Neurosci.* 2002, *18*, 15-27.

[11] Bauer, W.; Briner, U.; Doepfner, W.; Haller, R.; Huguenin, R.; Marbach, P.; Petcher, T. J.; Pless, J. SMS 201-995: A very potent and selective octapeptide analogue of somatostatin with prolonged action. *Life Sciences* 1982, *31*, 1133-1140.

[2] a) O'Byrne, K. J.; Halmos, G.; Pinski, J.; Groot, K.; Szepeshazi, K.; Shally, A. V.; Carney, D. N. Somatostatin receptor expression in lung cancer. *Eur. J. Cancer*. 1994, *30*, 1682-1687. b) Reubi, J. C.; Waser, B.; Schaer, J. C.; Laissue, J. A. Somatostatin receptor sst1-5 expression in normal and neoplastic human tissues using receptor autoradiography with subtype-selective ligands. *Eur. J. Nucl. Med*. 2001, *28*, 836-846. c) Callison, J. C.; Walker, R. C.; Massion, P. P. Somatostatin receptors in lung cancer: From function to molecular imaging and therapeutics. *J. Lung Cancer* 2011, 10, 69-76. d) Barbieri, F.; Bajetto, A.; Pattarozzi, A; Gatti, M.; Würth, R.; Thellung, S.; Corsaro, A.; Villa, V.; Nizzari, M.; Florio, T. Peptide receptor targeting in cancer: The somatostatin paradigm. *Int. J. Pept*. 2013, Article ID 926295, https://doi.org/10.1155/2013/926295

[3] a) de Herder, W. W.; Hofland, L. J.; van der Lely, A. J.; Lamberts, S. W. J. Somatostatin receptors in gastroentero-pancreatic neuroendocrine tumors. *Endocrine-*

Related Cancer 2003, *10*, 451-458. b) Öberg, K. E. Reubi, J. C.; Kwekkeboom, D. J.; Krenning, E. P. Role of somatostatins in gastroenteropancreatic neuroendocrine tumor development and therapy. *Gastroenterology* 2010, *139*, 742-753.

[4] Hofland, J. J.; Lamberts, S. W. J. Somatostatin receptor subtype expression in human tumors. *Annals of Oncology* 2001, *12*, S31-S36.

[5] Cescato, R.; Schulz, S.; Waser, B.; Eltschinger, V.; Rivier, J. E.; Wester, H.-J.; Culler, M.; Ginj, M.; Liu, Q.; Schonbrunn, A.; Reubi, J. C. Internalization of sst2, sst3, and sst5 receptors: Effects of somatostatin agonists and antagonists. *J. Nucl. Med*. 2006, *47*, 502-511.

[6] a) Nagy, A.; Schally, A. V.; Halmos, G.; Armatis, P.; Cai, R.-Z.; Csernus, V.; Kovács, M.; Koppán, M.; Szepesházi, K.; Kahán, Z. Synthesis and biological evaluation of cytotoxic analogs of somatostatin containing doxorubicin or its intensely potent derivative, 2-pyrrolinodoxorubicin. *Proc. Natl. Acad. Sci*. 1998, *95*, 1794-1799. b) Sun, L.-C.; Luo, J.; Mackey, V.; Fuselier, J. Coy, D. H. A conjugate of camptothecin and a somatostatin analog against prostate cancer cell invasion via a possible signaling pathway involving

PI3K/Akt, αVβ3/αVβ5 and MMP-2/-9. *Cancer Letters* 2007, *246*, 157-166. c) Delpassand, E. S.; Samarghandi, A.; Zamanian, S.; Wolin, E. M.; Hamiditabar, M.; Espenan, G. D.; Erion, J. L.; O'Dorisio, T. M.; Kvols, L. K.; Simon, J.; Wolfangel, R.; Camp, A.; Krenning, E. P.; Mojtahedi, A. Peptide receptor radionuclide therapy with 177Lu-DOTATATE for patients with somatostatin receptor-expressing neuroendocrine tumors: The first US phase 2 experience. *Pancreas* 2014, *43*, 518-525. d) Redko, B.; Ragozin, E.; Andreii, B.; Helena, T.; Amnon, A; Talia, S. Z.; Mor, O.-H., Genady, K.; Gary, G. Synthesis, drug release, and biological evaluation of new anticancer drug–bioconjugates containing somatostatin backbone cyclic analog as a targeting moiety. *Biopolymers* 2015, *104*, 743-752. e) Ragozin, E.; Hesin, A.; Bazylevich, A.; Tuchinsky, H.; Bovina, A.; Shekhter Zahavi, T.; Oron-Herman, M.; Kostenich, G.; Firer, M. A.; Rubinek, T.; Wolf, I.; Luboshits, G.; Sherman, M. Y.; Gellerman, G. New somatostatin-drug conjugates for effective targeting pancreatic cancer. *Bioorg. Med. Chem.* 2018, *26*, 3825-3836.

[7] Widdison, W. C.; Wilhelm, S. D.; Cavanagh, E. E.; Whiteman, K. R.; Leece, B. A.; Kovtun, Y.; Goldmacher, V. S.; Xie, H.; Steeves, R. M.; Lutz, R. J.; Zhao, R.; Wang, L.;

Blättler, W. A.; Chari, R. V. J. Semisynthetic maytansine analogues for the targeted treatment of cancer. *J. Med. Chem.* 2006, *49*, 4392-4408.

[8] Bouchet, B. P.; Galmarini, C. M. Cabazitaxel, a new taxane with favorable properties. *Drugs Today* 2010, *46*, 735-742.

[9] Doronina, S. O.; Toki, B. E.; Torgov, M. Y.; Mendelsohn, B. A.; Cerveny, C. G.; Chace, D. F.; DeBlanc, R. L.; Gearing, R. P.; Bovee, T. D.; Siegall, C. B.; Francisco, J. A.; Wahl, A. F.; Meyer, D. L.; Senter, P. D. Development of potent monoclonal antibody auristatin conjugates for cancer therapy. *Nature Biotechnology* 2003, *21*, 778-784.

[20] Henne, W. A.; Doorneweerd, D. D.; Hilgenbrink, A. R.; Kularatne, S. A.; Low, P. S. Synthesis and activity of a folate peptide camptothecin prodrug. *Bioorg. Med. Chem. Lett.* 2006, *16*, 5350-5355.

[21] Omelyanenko, V.; Gentry, C.; Kopečovà, P.; Kopeček, J. HPMA copolymer-anticancer drug-OV-TL16 antibody conjugates. II. Processing in epithelial ovarian carcinoma cells in vitro. *Int. J. Cancer* 1998, *75*, 600-608.

[22] Cai, R.-Z.; Szoke, B.; Lu, R.; Fu, D.; Redding, T. W.; Schally, A. V. Synthesis and biological activity of highly potent octapeptide analogs of somatostatin. *Proc. Natl. Acad. Sci.* 1986, *83*, 1896-1900.

[23] Cyr, J. E.; Pearson, D. A.; Wilson, D. M.; Nelson, C. A.; Guaraldi, M.; Azure, M. T.; Lister-James, J.; Dinkelborg, L. M.; Dean, R. T. Somatostatin receptor-binding peptides suitable for tumor radiotherapy with Re-188 or Re-186. Chemistry and initial biological studies. *J. Med. Chem.* 2007, *50*, 1354-1364.

[24] Reubi, J. C.; Schär, J.-C.; Waser, B.; Wenger, S.; Heppeler, A.; Schmitt, J.; Mäcke, H. R. Affinity profiles for human somatostatin receptor subtypes sst1-sst5 of somatostatin radiotracers selected for scintigraphic and radiotherapeutic use. *Eur. J. Nucl. Med.* 2000, *27*, 273-282.

[25] Kellogg, B. A.; Garrett, L.; Kovtun, Y.; Lai, K. C.; Leece, B.; Miller, M.; Payne, G.; Steeves, R; Whiteman, K. R.; Widdison, W.; Xie, H.; Singh, R.; Chari, R. V. J.; Lambert, J. M.; Lutz, R. J. Disulfide-linked antibody-maytansinoid conjugates: Optimization of in

vivo activity by varying the steric hinderance at carbon atoms adjacent to the disulfide linkage. *Bioconj. Chem.* 2011, *22*, 717-727.

Table of contents graphic: